



LLMs in utilizing molecular representations and adapting to various tasks.

Several prior studies [22, 35, 49] have undertaken the endeavor of fine-tuning generalist LLMs to develop foundational models within the molecular domain. Despite their enhancement to the original generalist LLM, these preceding works have unveiled several **issues**:

1. Insufficient alignment between modalities.
2. The consideration of an optimal molecular structure encoder remains unexplored.
3. A rudimentary design of the training pipeline neglects the update of LLMs’ knowledge.

These extant issues lead to a significant disparity in the performance of the current AI assistants across various practical tasks when compared to traditional specialist models.

To address these problems, we introduce **InstructMol** (Figure 2), a multi-modality instruction-tuning-based LLM. This model aligns molecular graphs and chemical sequential modalities with the natural language of humans. Through the utilization of a calibrated collection of molecule-related instruction datasets and a two-stage training scheme, **InstructMol** effectively leverages the pre-trained LLM and molecule graph encoder for molecule-text alignment. In the first alignment pretraining stage, we employ molecule-description pairs to train a lightweight and adaptable interface, which is designed to project the molecular node-level representation into the textual space that can be understood by the LLM. Subsequently, we finetune with multiple task-specific instructions. During this process, we freeze the molecule graph encoder and train a low-rank adapter (LoRA [24]) on the LLM to adapt our model to various scenarios. This efficient approach enables the seamless integration of molecular and textual information, promoting the development of versatile and robust cognitive abilities in the molecular domain.

To illustrate the capabilities of our model, we perform experiments that span three facets of drug discovery-related tasks, including compound property prediction, molecule description generation, and analysis of chemical reactions involving compounds. These tasks serve as robust benchmarks to assess the model’s ability to deliver useful and accurate knowledge feedback in practical drug discovery scenarios. The results in all experiments consistently indicate that our model significantly improves the performance of LLMs in tasks related to the understanding and design of molecular compounds. Consequently, this advance effectively reduces the disparity with specialized models. Our main contributions can be summarized as follows:

- We introduce **InstructMol**, a molecular-related multi-modality LLM, representing a pioneering effort in bridging the gap between molecular and textual information.
- In the context of a scarcity of high-quality annotated data in the drug discovery domain, our approach strives to efficiently extract molecular representations (targets on **Issue2**).

Employing a two-stage instruction tuning paradigm enhances the LLM’s understanding of molecular structural and sequential knowledge (targets on **Issue1** and **Issue3**).

- We evaluate our model through multiple practical assessments, demonstrating its substantial improvement compared to state-of-the-art LLMs. Our work lays the foundation for creating a versatile and reliable molecular research assistant in the drug discovery domain.

## 2. Related Work

### 2.1. Multimodal Instruction Tuning

There have been notable advancements in LLMs [9, 19–21, 50, 68] achieved through scaling up model and data size. Consequently, LLMs have shown remarkable performances in zero/few-shot NLP tasks [50, 52, 74]. A key technique in LLMs is instruction tuning, where pre-trained LLMs are fine-tuned on instruction-formatted datasets [74], allowing them to generalize to new tasks. Recently, with the emergence of large foundation models in various domains, several efforts have been made to transition from unimodal LLMs to multimodal LLMs (MLLMs) [4, 38, 51, 81, 87]. The primary research on multimodal instruction tuning (M-IT) includes the following [82]: *Constructing effective M-IT datasets* (adapting existing benchmarks datasets [13, 38, 87] or using self-instruction [32, 38, 70, 85]), *Bridging diverse modalities* (project-based [32, 38, 54] and query-based [70, 81, 87]) and *Employing reliable evaluation methods* (GPT-scoring [8, 32, 38, 47], manual scoring [80, 81], or closed-set measurement [8, 13, 32, 38, 47, 87, 87]). Most current MLLM research focuses on integrating vision and language while combining other modalities (e.g., graphs [39, 65]) with natural language remains nascent.

### 2.2. Molecule Foundation Models

The foundation models, trained on vast unlabeled data, serve as a paradigm for adaptable AI systems across diverse applications. Recently, the rise of vision and language pre-training [15, 46, 55] has sparked advancements in Molecule Foundation Models (MolFM). This includes approaches involving training in a single modality or jointly learning from multiple modalities. In the single modality domain, researchers are exploring the molecule representations from diverse sources, such as 1D sequences (e.g., SMILES [10, 26, 69]), 2D molecular graphs [25, 72, 83], 3D geometric conformations [41, 63, 63], or textual information from biomedical literature [6, 23, 31]. In the realm of multimodal analysis, research initiatives employ diverse approaches. These include encoder-decoder models to establish intermodal bridges [11, 18, 44], joint generative modeling of SMILES and textual data [84], and the adoption of contrastive learning for integrating molecular knowledge across varying modalities [40, 42, 48, 64].

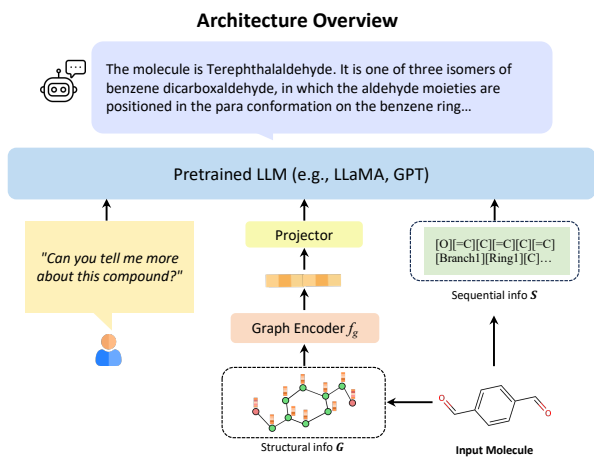


Figure 2. Overview of **InstructMol** model architecture design and two-stage training paradigm. The example molecule in the figure is *Terephthalaldehyde* [62] (CID 12173).

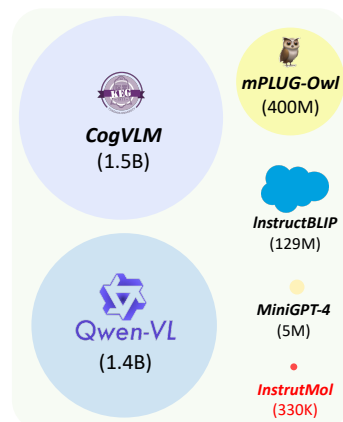
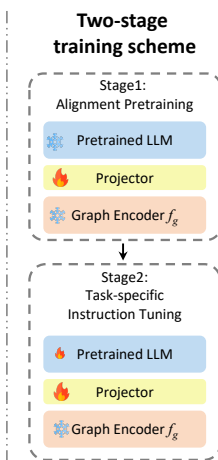


Figure 3. Comparison of biomolecule-domain molecule-text dataset scale with existing general domain vision-language datasets [4, 13, 71, 81, 87].

### 2.3. Molecule-related LLMs

Given the rapid progress in LLMs, some researchers are considering developing ChatGPT-like AI systems for drug discovery. Their goal is to offer guidance for optimizing lead compounds, accurately predicting drug interactions, and improving the comprehension of structure-activity relationships [35]. Several initiatives have already commenced to create instruction datasets within the biomolecular domain [22]. They aim to utilize instruction tuning techniques to enable LLMs, initially trained on general domain data, to acquire knowledge about biomolecular science [49, 76]. Additionally, other researchers are investigating methods to align structural data with textual information, bridging the gap between biological data and natural language [35, 49].

**Remark.** Our work lies in the intersection of molecule foundation models and multimodal LLM. It employs an efficient molecule graph encoder to parse structural information and integrates both structural and sequential details into a generalist LLM. **InstructMol** enables the LLM to understand molecule representations and apply its robust generalization to diverse molecular tasks.

## 3. Method

### 3.1. Preliminary of M-IT

Instruction tuning refers to finetuning pretrained LLMs on instruction datasets, enabling generalization to specific tasks by adhering to new instructions. Multi-modality instruction tuning (M-IT) integrates modalities like images and graphs into an LLM, expanding the model’s capability to accommodate multiple modalities.

A multimodal instruction tuning sample comprises an instruction  $I$  (e.g., "Describe the compound in detail") and an input-output pair. In the context of our study, the input

is one or more modalities derived from a molecule (e.g., molecule graph and sequence information), collectively denoted as  $M$ . The output  $R$  represents the textual response to the instruction conditioned on the input. The model aims to predict an answer given the instruction and multimodal input:  $\tilde{R} = f(I, M; \theta)$ , where  $\theta$  are the parameters of MLLM. The training objective is typically the same auto-regressive objective as the LLM pre-training stage, which can be expressed as:

$$\mathcal{L}(\theta) = - \sum_{i=1}^L \log p(R_i | I, M, R_{<i}; \theta), \quad (1)$$

where  $L$  is the target  $R$ ’s token length.

### 3.2. Construction of Molecular Instruction

**Data Collection.** In the field of biomolecular research, there is a noticeable scarcity of molecular datasets with comprehensive text annotations when compared to the vision-language domain, as depicted in Figure 3. While it is possible to construct instruction datasets in general domains by adapting benchmarks or using self-instruction, the application of these methods in the biomolecular domain presents challenges. This difficulty arises from two main factors: 1) biomolecular domain annotation demands expert knowledge and entails substantial complexity; 2) the knowledge within this domain spans a broad range of subjects, including structural biology, computational chemistry, drug sources, and chemical synthesis processes.

In our efforts, we have gathered recent open-access text-molecule pairs datasets and also independently constructed a portion of instruction data suitable for property prediction. Table 1 illustrates the composition of the data utilized during the two-stage training process.

**Molecule Input.** We utilize both the structure and sequence information of a molecule. We encode the structural informa-

TASKS	# SAMPLES	DATA SOURCE
Alignment Pretrain	264K	PubMed [29]
Property Prediction(Regression)	362K	QM9 [22, 77]
Property Prediction(Classification)	35,742	BACE, BBBP, HIV [77]
Molecule Description Generation	26,507	ChEBI-20 [17]
Forward Prediction	125K	USPTO [22, 73]
Retrosynthesis	130K	USPTO_500MT [22, 45]
Reagent Prediction	125K	USPTO_500K [22, 45]

Table 1. Details of InstructMol two-stage training data.

tion of a molecule as a graph, denoted by  $\mathcal{G} = (\mathcal{V}, \mathcal{E}, \mathcal{A}, \mathcal{X})$ , where  $\mathcal{V}$  is the set of atoms (nodes) and  $|\mathcal{V}| = N$  is the total number of atoms. The set of edges  $\mathcal{E}$  includes all chemical bonds, and  $\mathcal{A} \in \mathbb{R}^{N \times N}$  is the adjacency matrix. Additionally,  $\mathcal{X} \in \mathbb{R}^{N \times F}$  encompasses attributes associated with each node, where  $F$  is the feature dimension. With a Graph Encoder  $f_g$ , we extract a graph representation  $\mathbf{Z}_G \in \mathbb{R}^{N \times d}$  at the node level, effectively describing the inherent structure of the molecule. Simultaneously, we consider encoding the sequential information of the molecule, denoted as  $S$ , as a supplementary source of structural information. To enhance the robustness of sequential molecular descriptors and mitigate syntactic and semantic invalidity present in SMILES [75], we employ SELFIES [30] as  $S$ , which is designed for mapping each token to a distinct structure or reference.

**Our Input Formulation.** We formulate a molecule-text pair ( $\mathbf{X}_M$  &  $\mathbf{X}_c$ ) to the corresponding instruction-following version like Human:  $\mathbf{X}_I <\text{mol}> \mathbf{X}_M <\text{STOP}> \backslash n$  Assistant:  $\mathbf{X}_A \backslash n$ . The  $\mathbf{X}_M$  represents the molecular representation, including the graph token  $\mathbf{X}_G$  and optionally the SELFIES token  $\mathbf{X}_S$ .  $\mathbf{X}_I$  denotes for instruction tokens and  $\mathbf{X}_A$  for answer tokens. For a given answer sequence of length  $L$ , our optimization objective is to maximize the probability of generating the target answers  $X_A$  by maximizing:

$$p(\mathbf{X}_A | \mathbf{X}_M, \mathbf{X}_I) = \prod_{i=1}^L p_{\theta}(x_i | \mathbf{X}_G \parallel \mathbf{X}_S, \mathbf{X}_I, \mathbf{X}_{A, <i)}). \quad (2)$$

To diversify  $\mathbf{X}_I$ , we craft clear task descriptions and use GPT-3.5-turbo to generate varied questions, enhancing instructions’ robustness. Note that we simply concatenate  $\mathbf{X}_G$  and  $\mathbf{X}_S$  along the length-dimension. More complex fusion methods require additional loss designs for supervision [40, 48], but here we prioritize simplicity.

### 3.3. Architecture

**Molecular Encoder.** The molecular graph-structure encoder,  $f_g$ , needs to effectively extract node representations while preserving the molecular graph’s connectivity information. It is crucial that  $f_g$  inherently establishes a pre-alignment in the representation space with the text space to facilitate

$\mathbf{Z}_G$  in the following alignment stage. Taking inspiration from common practices in the Vision Large Language Models (VLLM) domain [4, 38, 81], where models like ViT initialized from CLIP [55] serve as vision encoders, we opt for MoleculeSTM’s graph encoder as  $f_g$  [42], instead of GraphMVP used by prior methodologies [35, 49]. The MoleculeSTM graph encoder model is obtained through molecular-textual contrastive training, mitigating the requirement for an extensive amount of paired data during training to align different modalities.

**Light-weight Alignment Projector.** In order to map graph features into the word embedding space, we utilize a trainable projection matrix  $\mathbf{W}$  to transform  $\mathbf{Z}_G$  into  $\mathbf{X}_G$ , ensuring that it has the same dimension as the word embedding space. Since the selected  $f_g$  has undergone partial alignment with the text through contrastive training, we believe a straightforward linear projection will meet the subsequent alignment needs. For approaches like gated cross-attention [2], Q-former [33], or position-aware vision-language adapters [4], they require a large number of pairs for pretraining alignment, which is typically unavailable in the biomolecular domain. We therefore do not explore these more complex alignment methods.

**Large Language Model.** InstructMol incorporates a pre-trained LLM as its foundational component. We opt for Vicuna-7B [9] as the initialized weights, which is derived from LLaMA [68] through supervised instruction finetuning.

### 3.4. Two-Stage of Instruction Tuning

As illustrated in Figure 2, the training process of InstructMol consists of two stages: alignment pretraining and instruction fine-tuning training.

**Alignment Pretraining.** In the first stage, we aim to align the modality of molecules with text, ensuring that the LLMs can perceive both the structural and sequential information of molecules and integrate molecular knowledge into their internal capabilities.

We primarily employ a dataset consisting of molecule-text pairs sourced from PubChem [29]. Each molecule structure is associated with a textual description elucidating chemical and physical properties or high-level bioactivity information. The construction of the PubChemDataset predominantly follows the MoleculeSTM [42] pipeline. We meticulously remove molecules with invalid descriptions and syntactic errors in their molecular descriptors. To ensure fairness, we also eliminate compounds that might appear in the downstream molecule-caption test set. This results in a dataset of 330K molecule-text pairs. Subsequently, we adopt a self-instruction-like approach to generate a diverse set of task descriptions as instructions.

During the training phase, to prevent overfitting and leverage pre-trained knowledge, we freeze both the graph encoder

and LLM, focusing solely on fine-tuning the alignment projector. After a few epochs of training, our aim is that the projector has successfully learned to map graph representations to graph tokens, aligning effectively with text tokens.

**Task-specific Instruction Tuning.** In the second stage, we target three distinct downstream scenarios. We advocate for task-specific instruction tuning to address the particular constraints inherent in various drug-discovery-related tasks. For *compound property prediction*, we utilize the quantum mechanics properties instruction dataset from [22] for regression prediction and the MoleculeNet dataset [77] for property classification. For *chemical reaction analysis*, we incorporate forward reaction prediction, retrosynthesis analysis, and reagent prediction tasks, all derived from [22]. To assess the model’s proficiency in translating between natural language and molecular expression, we integrate ChEBI-20 [17] for the *molecule description generation task*. For each task, corresponding instruction templates are designed.

During the training process, we utilize the parameters of the alignment projector that were trained in the first stage as initialization. We only keep the molecular encoder  $f_g$  frozen and continue to update the pre-trained weights of the projector and the LLM. To adapt the LLM effectively for diverse tasks, we employ low-rank adaptation (i.e., LoRA [24]), opting against full-tuning to mitigate potential forgetting issues. In practical applications, we have the flexibility to substitute different adaptors based on specific scenario requirements or combine multiple adaptors to integrate knowledge, thereby showcasing the model’s modularization capabilities. Moreover, LoRA adaptation allows the LLM to retain the inherent capacity for common-sense reasoning in dialogue.

## 4. Implementations

**Model Settings.** A graph neural network with five graph isomorphism network (GIN) [79] layers is used as the molecule graph encoder  $f_g$ . The hidden dimension is set to be 300. The GIN model is initialized using the MoleculeSTM [42] graph encoder, which is pre-trained through molecular graph-text contrastive learning. We employ Vicuna-v-1.3-7B [9] as the base LLM, which has been trained through instruction-tuning. The total number of parameters of InstructMol is around 6.9B. More specifically, **InstructMol+GS** denotes we inject both molecular graph tokens and sequence tokens into the input, while **InstructMol+G** means only incorporates graph tokens.

**Training Details.** In the first stage, we employ the training split comprising around 264K molecule-caption pairs from PubMed. Using a batch size of 128, we conduct training for 5 epochs. We use the AdamW optimizer, with  $\beta=(0.9, 0.999)$  and a learning rate of  $2e-3$ , without weight decay. Warm-up is executed over 3% of the total training steps, followed by a cosine schedule for learning rate decay. For the second

stage, we conduct training for three specific scenarios. For fair comparisons with traditional methods, training spans 20 to 50 epochs for the molecule description generation task using the ChEBI-20 training split. Property prediction and reaction tasks undergo 10 epochs using corresponding instruction datasets. In InstructMol training, we maintain a consistent batch size of 128 and set the learning rate to  $8e-5$ . Linear layers within the LLM utilize a LoRA rank of 64 and a scaling value  $\alpha$  of 16. All experiments are run with  $4\times$  RTX A6000 (48GB) GPUs.

## 5. Experiments

### 5.1. Property Prediction Task

**Experiment Setup.** Property prediction intends to forecast a molecule’s intrinsic physical and chemical properties from its structural or sequential characteristics. In the context of the regression task, we undertake experiments on the Property Prediction dataset from [22], where the objective is to predict the quantum mechanic’s properties of a given molecule, specifically including HUMO, LUMO, and the HUMO-LUMO gap [58]. For the classification task, we incorporate three binary classification datasets pertaining to molecular biological activity, namely BACE, BBBP, and HIV. In classification, all dataset samples are converted into an instruction format and we use the recommended splits from [59]. Each item comprises an instruction explaining the property for prediction and the representation of the molecule. Subsequently, models are tasked with generating a single prediction (“yes” or “no”).

**Results.** Our model trains on the provided split and is compared against baselines on the test set for regression, measured by Mean Absolute Error (MAE) in Table 2. Compared to previous single-modal instruction-tuned LLM-based methods [22], InstructMol demonstrates a further improvement in the regression task. ROC-AUC scores for classification outcomes are presented in Table 3. In comparison to LLM-based generalist models, both the Galactica [67] series models trained on an extensive scientific literature dataset and the single-modality LLM fine-tuned with task-specific instructions [22], InstructMol demonstrates consistent improvements in accuracy across the three task datasets. However, we observe that our predictive results still exhibit some disparity compared to expert models [41, 86] specifically trained on a vast molecule structure dataset.

### 5.2. Molecule Description Generation Task

**Experiment Setup.** Molecule description generation encapsulates a comprehensive depiction of a molecule, covering its structure, properties, biological activity, and applications based on molecular descriptors. This task is more complex than classification or regression, providing a robust measure of the model’s understanding of molecules. We convert the

METHOD	HOMO ↓	LUMO ↓	$\Delta\epsilon$ ↓	AVG ↓
<i>LLM Based Generalist Models</i>				
Alpaca <sup>†</sup> [66]	-	-	-	322.109
Baize <sup>†</sup> [78]	-	-	-	261.343
LLama2-7B [20] (5-shot ICL)	0.7367	0.8641	0.5152	0.7510
Vicuna-13B [9] (5-shot ICL)	0.7135	3.6807	1.5407	1.9783
Mol-Instruction [22]	0.0210	0.0210	0.0203	0.0210
<b>InstructMol-G</b>	0.0060	0.0070	0.0082	0.0070
<b>InstructMol-GS</b>	<b>0.0048</b>	<b>0.0050</b>	<b>0.0061</b>	<b>0.0050</b>

Table 2. Results of molecular property prediction tasks (regression) on QM9. We report the result in MAE (hartree). †: few-shot in-context learning (ICL) results from [22].  $\Delta\epsilon$ : HOMO-LUMO energy gap.

METHOD	BACE ↑	BBBP ↑	HIV ↑
# MOLECULES	1513	2039	41127
<i>Specialist Models</i>			
KV-PLM [84]	78.5	70.5	71.8
GraphCL [83]	75.3	69.7	78.5
GraphMVP-C [41]	81.2	72.4	77.0
MoMu [64]	76.7	70.5	75.9
MolFM [48]	83.9	<b>72.9</b>	78.8
Uni-Mol [86]	<b>85.7</b>	<b>72.9</b>	<b>80.8</b>
<i>LLM Based Generalist Models</i>			
Galactica-6.7B [67]	58.4	53.5	72.2
Galactica-30B [67]	72.7	59.6	<b>75.9</b>
Galactica-120B [67]	61.7	66.1	74.5
Vicuna-v1.5-13b-16k (4-shot) [9]	49.2	52.7	50.5
Vicuna-v1.3-7b* [9]	68.3	60.1	58.1
LLama-2-7b-chat* [20]	74.8	65.6	62.3
<b>InstructMol-G</b>	<b>85.9</b>	64.0	74.0
<b>InstructMol-GS</b>	82.3	<b>70.0</b>	68.9

Table 3. ROC-AUC results of molecular property prediction tasks (classification) on MoleculeNet [77] benchmarks. \*: use LoRA tuning.

training subset of the ChEBI-20 dataset [17] into an instructional format and subsequently perform fine-tuning based on these instructions. Assessment is carried out using evaluation metrics aligned with [18].

**Baselines.** There exist various models, including 1) MolT5-like expert models [18, 43] and a multitude of models employing MolT5 as a decoder [11, 40, 48, 64], 2) models based on retrieval methods that utilize ChatGPT/GPT-4 as a foundational component [34], 3) other models derived through instruction-tuning with LLMs to achieve generalist unimodal [22] and multi-modalities [49] capabilities.

**Results.** Table 4 presents the overall results for molecule description generation. Our model outperforms other generalist LLM-based models in generating precise, contextually relevant molecule descriptions. We observe that incorporating both molecule structural information and sequential information in the input yields higher-quality results ( $\sim 2\%$  improvement) than providing structural information alone. While expert models demonstrate better efficacy in comparison, it is noteworthy that they are constrained by their training schemes and lack the versatile capabilities inherent in our approach. Retrieval methods, supported by ChatGPT/GPT-4, demonstrate strong capabilities. Our future efforts will focus on integrating these methods to improve the accuracy and credibility of generated content.

### 5.3. Chemical Reaction-related task

**Experiment Setup.** Traditionally, identifying chemical reactions relied on intuition and expertise. Integrating deep learning for predicting reactions can accelerate research and improve drug discovery. The general format of a chemical reaction is "reactant  $\rightarrow$  reagent  $\rightarrow$  product". Here we mainly focus on three tasks: 1) *Forward Reaction Prediction*: predict the probable product(s) given specific reactants and reagents; 2) *Reagent Prediction*: ascertain the suitable catalysts, solvents, or ancillary substances required for a specific chemical reaction given reactant(s) and product(s); 3) *Retrosynthesis*: anticipate deducing potential precursor molecule(s) from given product(s).

We utilize the dataset sourced from [22], training it on the pre-defined training split, and subsequently evaluating its performance on the test set. The performance is assessed by metrics like Fingerprint Tanimoto Similarity (FTS), BLEU, Exact Match and Levenshtein distance to measure the similarity between ground truth and prediction. We also measure the validity of predicted molecules using RDKit.

**Results.** Table 5 reports the outcomes of tasks related to chemical reactions. It is evident that **InstructMol** outperforms the baselines by a significant margin. The results obtained by generalist LLMs are derived from [22], and they exhibit a pronounced inability to comprehend any chemical reaction prediction task, struggling to generate valid molecule(s) as answers. Mol-Instruction [22], employing Llama2 [20] as the base LLM, is jointly trained on multiple molecule-oriented instruction datasets. In addition, we supplement this by adopting the same training settings but exclusively training on chemical reaction-related datasets. Through comparison, InstructMol, representing a multi-modality LLM, demonstrates a superior understanding of the task compared to single-modality models, confirming its effectiveness as a chemical reaction assistant.

### 5.4. Qualitative Analysis

Several examples of different task results are shown in Figure 4. Figure 4 (a-c) demonstrate the remarkable proficiency of InstructMol in accurately generating compounds related to chemical reaction prediction tasks. In Figure 4 (d), InstructMol produces captions that closely match the ground truth, providing an accurate description of the **family** (i.e. "a member of the class of indole-3-acetic acids"), **structure** (i.e. "the hydrogen at position 5 has been replaced by a carboxy group") and **biological activity** (i.e. "It has a role as a bacterial metabolite.").

### 5.5. Ablation Studies

In this subsection, we conduct an ablation study to investigate the architecture and training scheme design of our proposed framework. We explore variations from several

MODEL	BLEU-2 $\uparrow$	BLEU-4 $\uparrow$	ROUGE-1 $\uparrow$	ROUGE-2 $\uparrow$	ROUGE-L $\uparrow$	METEOR $\uparrow$
<i>Specialist Models</i>						
MoT5-base [18]	0.540	0.457	0.634	0.485	0.568	0.569
MoMu (MolT5-base) [64]	0.549	0.462	-	-	-	0.576
MolFM (MolT5-base) [48]	0.585	0.498	0.653	0.508	0.594	0.607
MolXPT [43]	0.594	0.505	0.660	0.511	0.597	0.626
GIT-Mol-graph [40]	0.290	0.210	0.540	0.445	0.512	0.491
GIT-Mol-SMILES [40]	0.264	0.176	0.477	0.374	0.451	0.430
GIT-Mol-(graph+SMILES) [40]	0.352	0.263	0.575	0.485	0.560	0.430
Text+Chem T5-augm-base [11]	<b>0.625</b>	<b>0.542</b>	<b>0.682</b>	<b>0.543</b>	<b>0.622</b>	<b>0.648</b>
<i>Retrieval Based LLMs</i>						
GPT-3.5-turbo (10-shot MolReGPT) [34]	0.565	0.482	0.623	0.450	0.543	0.585
GPT-4-0314 (10-shot MolReGPT) [34]	0.607	0.525	0.634	0.476	0.562	0.610
<i>LLM Based Generalist Models</i>						
GPT-3.5-turbo (zero-shot) [34]	0.103	0.050	0.261	0.088	0.204	0.161
BioMedGPT-10B [49]	0.234	0.141	0.386	0.206	0.332	0.308
Mol-Instruction [22]	0.249	0.171	0.331	0.203	0.289	0.271
<b>InstructMol-G</b>	0.466	0.365	0.547	0.365	0.479	0.491
<b>InstructMol-GS</b>	<b>0.475</b>	<b>0.371</b>	<b>0.566</b>	<b>0.394</b>	<b>0.502</b>	<b>0.509</b>

Table 4. Results of molecular description generation task on the test split of ChEBI-20.

MODEL	EXACT $\uparrow$	BLEU $\uparrow$	LEVENSHTEIN $\downarrow$	RDk FTS $\uparrow$	MACCS FTS $\uparrow$	MORGAN FTS $\uparrow$	VALIDITY $\uparrow$
<i>Reagent Prediction</i>							
Alpaca $\dagger$ [66]	0.000	0.026	29.037	0.029	0.016	0.001	0.186
Baize $\dagger$ [78]	0.000	0.051	30.628	0.022	0.018	0.004	0.099
ChatGLM $\dagger$ [19]	0.000	0.019	29.169	0.017	0.006	0.002	0.074
LLama $\dagger$ [68]	0.000	0.003	28.040	0.037	0.001	0.001	0.001
Vicuna $\dagger$ [9]	0.000	0.010	27.948	0.038	0.002	0.001	0.007
Mol-Instruction [22]	0.044	0.224	23.167	0.237	0.364	0.213	1.000
LLama-7b* [68](LoRA)	0.000	0.283	53.510	0.136	0.294	0.106	1.000
<b>InstructMol-G</b>	0.070	<b>0.890</b>	24.732	<b>0.469</b>	<b>0.691</b>	<b>0.426</b>	1.000
<b>InstructMol-GS</b>	<b>0.129</b>	0.610	<b>19.664</b>	0.444	0.539	0.400	1.000
<i>Forward Reaction Prediction</i>							
Alpaca $\dagger$ [66]	0.000	0.065	41.989	0.004	0.024	0.008	0.138
Baize $\dagger$ [78]	0.000	0.044	41.500	0.004	0.025	0.009	0.097
ChatGLM $\dagger$ [19]	0.000	0.183	40.008	0.050	0.100	0.044	0.108
LLama $\dagger$ [68]	0.000	0.020	42.002	0.001	0.002	0.001	0.039
Vicuna $\dagger$ [9]	0.000	0.057	41.690	0.007	0.016	0.006	0.059
Mol-Instruction [22]	0.045	0.654	27.262	0.313	0.509	0.262	1.000
LLama-7b* [68](LoRA)	0.012	0.804	29.947	0.499	0.649	0.407	1.000
<b>InstructMo-G</b>	0.153	0.906	20.155	0.519	0.717	0.457	1.000
<b>InstructMol-GS</b>	<b>0.536</b>	<b>0.967</b>	<b>10.851</b>	<b>0.776</b>	<b>0.878</b>	<b>0.741</b>	1.000
<i>Retrosynthesis</i>							
Alpaca $\dagger$ [66]	0.000	0.063	46.915	0.005	0.023	0.007	0.160
Baize $\dagger$ [78]	0.000	0.095	44.714	0.025	0.050	0.023	0.112
ChatGLM $\dagger$ [19]	0.000	0.117	48.365	0.056	0.075	0.043	0.046
LLama $\dagger$ [68]	0.000	0.036	46.844	0.018	0.029	0.017	0.010
Vicuna $\dagger$ [9]	0.000	0.057	46.877	0.025	0.030	0.021	0.017
Mol-Instruction [22]	0.009	0.705	31.227	0.283	0.487	0.230	1.000
LLama-7b* [68](LoRA)	0.000	0.283	53.510	0.136	0.294	0.106	1.000
<b>InstructMol-G</b>	0.114	0.586	21.271	0.422	0.523	0.285	1.000
<b>InstructMol-GS</b>	<b>0.407</b>	<b>0.941</b>	<b>13.967</b>	<b>0.753</b>	<b>0.852</b>	<b>0.714</b>	1.000

Table 5. Results of chemical reaction tasks. These tasks encompass reagent prediction, forward reaction prediction, and retrosynthesis.  $\dagger$ : few-shot ICL results from [22]. \*: use task-specific instruction data to finetune.

perspectives and validate them on the task of molecule description generation. The ablation results are presented in the Table 6 as follows: **1) Employing an MLP connector instead of a linear projector.** Drawing inspiration from the observations made in [37], we attempt to change the alignment projector to a two-layer MLP, demonstrating an enhancement in the model’s multimodal capabilities. **2) Scaling up the LLM to 13B.** The results indicate that scaling up the LLM only yields minor improvements. Thus, it substantiates the assertion that, for specific domains characterized by dataset scarcity, employing a 7B size model is sufficiently efficient for modeling. **3) Replacing the graph encoder  $f_g$**

**with a single-modality module** (i.e., GraphMVP [41] with the same parameter size and architecture as we used). The results affirm our perspective: utilizing an encoder pre-aligned with text enhances the effectiveness of modality alignment. **4) Freezing the LLM in the second stage.** Adopting a strategy akin to BioMedGPT10B [49] and DrugChat [35], we choose not to update LLM weights in the second stage. The training outcomes reveal challenges in convergence and an inability to complete normal inference, thus demonstrating the necessity for the instruct-tuning stage to adapt LLM knowledge to the specific task.

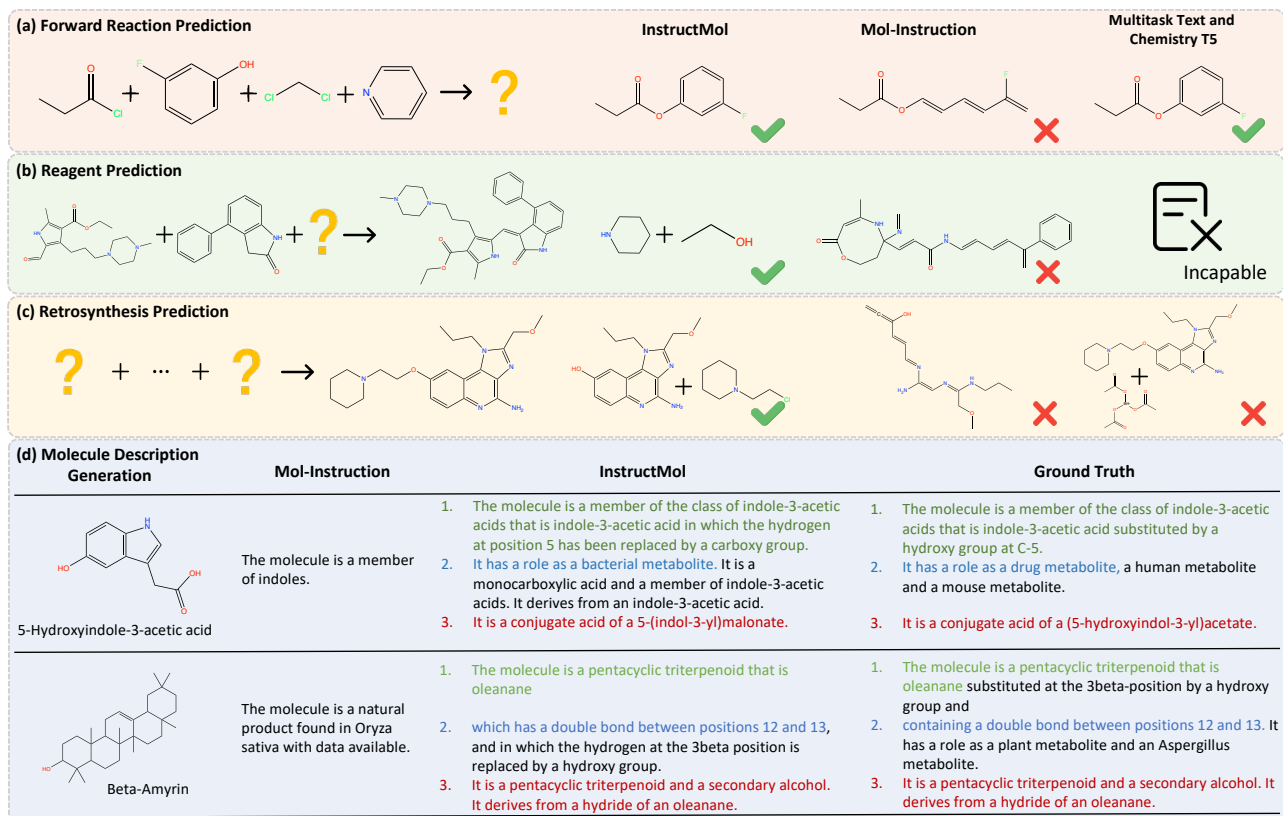


Figure 4. Comparison of chemical reaction and molecule description generation tasks results. (a-c) demonstrate the performance relative to baselines [11, 22], highlighting InstructMol’s precise generation of reaction-related compounds. (d) reveals InstructMol’s caption aligning closely with the ground truth. The colored text represents the exact match between the output of InstructMol and the ground truth.

METHODS	BLEU-2 $\uparrow$	BLEU-4 $\uparrow$	ROUGE-1 $\uparrow$	ROUGE-2 $\uparrow$	ROUGE-L $\uparrow$	METEOR $\uparrow$
<b>InstructMol+G</b>	0.4620	0.3560	0.5439	0.3644	0.4765	0.4832
+MLP XL connector	<b>0.4665(+0.97%)</b>	<b>0.3613(+1.49%)</b>	<b>0.5497(+1.07%)</b>	<b>0.3699(+1.51%)</b>	<b>0.4805(+0.84%)</b>	<b>0.4917(+1.76%)</b>
+Scale up LLM	0.4615(-0.11%)	0.3566(+0.17%)	0.5449(+0.18%)	0.3660(+0.44%)	0.4776(+0.23%)	0.4868(+0.75%)
Replace $f_g$ with GraphMVP [41]	0.4452(-3.64%)	0.3377(-5.14%)	0.5318(-0.11%)	0.3484(-2.22%)	0.4638(-2.67%)	0.4691(-2.92%)
Freeze LLM in the second stage	-	-	-	-	-	-

Table 6. Ablation of the model architecture and training scheme design. We chose to conduct experiments on the Molecule Description Generation task.  $f_g$  represents the molecule graph encoder. All experiments are trained with 20 epochs.

## 6. Discussion and Conclusion

**Conclusion.** This study introduces InstructMol, a pioneering multi-modality foundational model designed to establish a connection between molecular modalities and human natural language. Through the incorporation of structural and sequential information of molecules into LLMs using a dual-stage alignment pre-training and instruction tuning paradigm, we facilitate the ability of the pre-trained general LLM to understand and interpret molecular information, particularly in tasks associated with drug discovery. The effectiveness of our model architecture and training approach is validated through extensive experimental evaluation, highlighting its potential for various practical applications in the field of drug discovery.

**Future Work.** Integrating multiple modalities with LLMs significantly enhances molecular research within this domain and is a valuable direction to explore. However, several challenges persist and require resolution. 1) *The scale and quality of relevant datasets lag behind those in the vision and language community.* Effectively extracting reliable annotations from experimental data remains a formidable obstacle. 2) *The lack of well-defined task objectives poses a challenge.* For instance, in the context of molecule description generation tasks, a meticulous examination of the accuracy of descriptions from various perspectives such as structure, property, and bioactivity is essential. 3) *A more scientifically robust evaluation is needed.* Addressing issues such as detecting the hallucinations in generation outputs to enhance safety presents a significant challenge.

## References

- [1] PubChem Structure Search. [https://pubchem.ncbi.nlm.nih.gov/search/help\\_search.html](https://pubchem.ncbi.nlm.nih.gov/search/help_search.html). 15
- [2] Jean-Baptiste Alayrac, Jeff Donahue, Pauline Luc, Antoine Miech, Iain Barr, Yana Hasson, Karel Lenc, Arthur Mensch, Katie Millican, Malcolm Reynolds, Roman Ring, Eliza Rutherford, Serkan Cabi, Tengda Han, Zhitao Gong, Sina Samangooei, Marianne Monteiro, Jacob Menick, Sebastian Borgeaud, Andy Brock, Aida Nematzadeh, Sahand Sharifzadeh, Mikolaj Binkowski, Ricardo Barreira, Oriol Vinyals, Andrew Zisserman, and Karen Simonyan. Flamingo: a visual language model for few-shot learning. *ArXiv*, abs/2204.14198, 2022. 4
- [3] Heba Askr, Enas Elgeldawi, Heba Aboul Ella, Yaseen A.M.M. Elshaiar, Mamdouh M. Gomaa, and Aboul Ella Hassanien. Deep learning in drug discovery: an integrative review and future challenges. *Artificial Intelligence Review*, 56:5975 – 6037, 2022. 1
- [4] Jinze Bai, Shuai Bai, Shusheng Yang, Shijie Wang, Sinan Tan, Peng Wang, Junyang Lin, Chang Zhou, and Jingren Zhou. Qwen-vl: A frontier large vision-language model with versatile abilities. *ArXiv*, abs/2308.12966, 2023. 2, 3, 4
- [5] Satantjeev Banerjee and Alon Lavie. Meteor: An automatic metric for mt evaluation with improved correlation with human judgments. In *EEvaluation@ACL*, 2005. 13
- [6] Iz Beltagy, Kyle Lo, and Arman Cohan. Scibert: A pre-trained language model for scientific text. In *Conference on Empirical Methods in Natural Language Processing*, 2019. 2
- [7] Tom B. Brown, Benjamin Mann, Nick Ryder, Melanie Subbiah, Jared Kaplan, Prafulla Dhariwal, Arvind Neelakantan, Pranav Shyam, Girish Sastry, Amanda Askell, Sandhini Agarwal, Ariel Herbert-Voss, Gretchen Krueger, T. J. Henighan, Rewon Child, Aditya Ramesh, Daniel M. Ziegler, Jeff Wu, Clemens Winter, Christopher Hesse, Mark Chen, Eric Sigler, Mateusz Litwin, Scott Gray, Benjamin Chess, Jack Clark, Christopher Berner, Sam McCandlish, Alec Radford, Ilya Sutskever, and Dario Amodei. Language models are few-shot learners. *ArXiv*, abs/2005.14165, 2020. 1
- [8] Feilong Chen, Minglun Han, Haozhi Zhao, Qingyang Zhang, Jing Shi, Shuang Xu, and Bo Xu. X-llm: Bootstrapping advanced large language models by treating multi-modalities as foreign languages. *ArXiv*, abs/2305.04160, 2023. 2
- [9] Wei-Lin Chiang, Zhuohan Li, Zi Lin, Ying Sheng, Zhanghao Wu, Hao Zhang, Lianmin Zheng, Siyuan Zhuang, Yonghao Zhuang, Joseph E. Gonzalez, Ion Stoica, and Eric P. Xing. Vicuna: An open-source chatbot impressing gpt-4 with 90%\* chatgpt quality, 2023. 2, 4, 5, 6, 7, 14
- [10] Seyone Chithrananda, Gabriel Grand, and Bharath Ramsundar. Chemberta: Large-scale self-supervised pretraining for molecular property prediction. *ArXiv*, abs/2010.09885, 2020. 2
- [11] Dimitrios Christofidellis, Giorgio Giannone, Jannis Born, Ole Winther, Teodoro Laino, and Matteo Manica. Unifying molecular and textual representations via multi-task language modelling. In *International Conference on Machine Learning*, 2023. 2, 6, 7, 8, 16, 18
- [12] Connor W. Coley. Defining and exploring chemical spaces. *Trends in Chemistry*, 2020. 1
- [13] Wenliang Dai, Junnan Li, Dongxu Li, Anthony Meng Huat Tiong, Junqi Zhao, Weisheng Wang, Boyang Albert Li, Pascale Fung, and Steven C. H. Hoi. Instructblip: Towards general-purpose vision-language models with instruction tuning. *ArXiv*, abs/2305.06500, 2023. 2, 3
- [14] Jacob Devlin, Ming-Wei Chang, Kenton Lee, and Kristina Toutanova. Bert: Pre-training of deep bidirectional transformers for language understanding. In *North American Chapter of the Association for Computational Linguistics*, 2019. 1
- [15] Zi-Yi Dou, Yichong Xu, Zhe Gan, Jianfeng Wang, Shuohang Wang, Lijuan Wang, Chenguang Zhu, Nanyun Peng, Zicheng Liu, and Michael Zeng. An empirical study of training end-to-end vision-and-language transformers. *2022 IEEE/CVF Conference on Computer Vision and Pattern Recognition (CVPR)*, pages 18145–18155, 2021. 2
- [16] Joseph L. Durant, Burton A. Leland, Douglas R. Henry, and James G. Nourse. Reoptimization of mdl keys for use in drug discovery. *Journal of chemical information and computer sciences*, 42 6:1273–80, 2002. 13
- [17] Carl N. Edwards, Chengxiang Zhai, and Heng Ji. Text2mol: Cross-modal molecule retrieval with natural language queries. In *Conference on Empirical Methods in Natural Language Processing*, 2021. 4, 5, 6, 13, 15
- [18] Carl N. Edwards, T. Lai, Kevin Ros, Garrett Honke, and Heng Ji. Translation between molecules and natural language. *ArXiv*, abs/2204.11817, 2022. 2, 6, 7, 13
- [19] Aohan Zeng et.al. GLM-130b: An open bilingual pre-trained model. In *The Eleventh International Conference on Learning Representations (ICLR)*, 2023. 2, 7
- [20] Hugo Touvron et.al. Llama 2: Open foundation and fine-tuned chat models. *ArXiv*, abs/2307.09288, 2023. 6, 14
- [21] Rohan Anil et.al. Palm 2 technical report. *ArXiv*, abs/2305.10403, 2023. 2
- [22] Yin Fang, Xiaozhuan Liang, Ningyu Zhang, Kangwei Liu, Rui Huang, Zhuo Chen, Xiaohui Fan, and Huajun Chen. Mol-instructions: A large-scale biomolecular instruction dataset for large language models. *ArXiv*, abs/2306.08018, 2023. 2, 3, 4, 5, 6, 7, 8, 13, 15, 16, 17, 18, 19
- [23] Yu Gu, Robert Tinn, Hao Cheng, Michael R. Lucas, Naoto Usuyama, Xiaodong Liu, Tristan Naumann, Jianfeng Gao, and Hoifung Poon. Domain-specific language model pre-training for biomedical natural language processing. *ACM Transactions on Computing for Healthcare (HEALTH)*, 3:1 – 23, 2020. 2
- [24] J. Edward Hu, Yelong Shen, Phillip Wallis, Zeyuan Allen-Zhu, Yuanzhi Li, Shean Wang, and Weizhu Chen. Lora: Low-rank adaptation of large language models. *ArXiv*, abs/2106.09685, 2021. 2, 5
- [25] Weihua Hu, Bowen Liu, Joseph Gomes, Marinka Zitnik, Percy Liang, Vijay S. Pande, and Jure Leskovec. Strategies for pre-training graph neural networks. *arXiv: Learning*, 2019. 2
- [26] Ross Irwin, Spyridon Dimitriadis, Jiazhen He, and Esben Jannik Bjerrum. Chemformer: a pre-trained transformer for computational chemistry. *Machine Learning: Science and Technology*, 3, 2021. 2

- [27] Jin Kim, Sera Park, Dongbo Min, and Wanky Kim. Comprehensive survey of recent drug discovery using deep learning. *International Journal of Molecular Sciences*, 22, 2021. [1](#)
- [28] Sunghwan Kim, Paul A. Thiessen, Tiejun Cheng, Jian Zhang, Asta Gindulyte, and Evan E. Bolton. Pug-view: programmatic access to chemical annotations integrated in pubchem. *Journal of Cheminformatics*, 11, 2019. [13](#)
- [29] Sunghwan Kim, Jie Chen, Tiejun Cheng, Asta Gindulyte, Jia He, Siqian He, Qingliang Li, Benjamin A. Shoemaker, Paul A. Thiessen, Bo Yu, Leonid Y. Zaslavsky, Jian Zhang, and Evan E. Bolton. Pubchem 2023 update. *Nucleic acids research*, 2022. [4](#), [13](#)
- [30] Mario Krenn, Florian Hase, AkshatKumar Nigam, Pascal Friederich, and Alán Aspuru-Guzik. Self-referencing embedded strings (selfies): A 100% robust molecular string representation. *Machine Learning: Science and Technology*, 1, 2019. [4](#)
- [31] Jinhyuk Lee, Wonjin Yoon, Sungdong Kim, Donghyeon Kim, Sunkyu Kim, Chan Ho So, and Jaewoo Kang. Biobert: a pre-trained biomedical language representation model for biomedical text mining. *Bioinformatics*, 36:1234 – 1240, 2019. [2](#)
- [32] Chunyuan Li, Cliff Wong, Sheng Zhang, Naoto Usuyama, Haotian Liu, Jianwei Yang, Tristan Naumann, Hoifung Poon, and Jianfeng Gao. Llava-med: Training a large language-and-vision assistant for biomedicine in one day. *ArXiv*, abs/2306.00890, 2023. [2](#)
- [33] Junnan Li, Dongxu Li, Silvio Savarese, and Steven C. H. Hoi. Blip-2: Bootstrapping language-image pre-training with frozen image encoders and large language models. *ArXiv*, abs/2301.12597, 2023. [4](#)
- [34] Jiatong Li, Yunqing Liu, Wenqi Fan, Xiao Wei, Hui Liu, Jiliang Tang, and Qing Li. Empowering molecule discovery for molecule-caption translation with large language models: A chatgpt perspective. *ArXiv*, abs/2306.06615, 2023. [6](#), [7](#)
- [35] Youwei Liang, Ruiyi Zhang, Li Zhang, and Peng Xie. Drugchat: Towards enabling chatgpt-like capabilities on drug molecule graphs. *ArXiv*, abs/2309.03907, 2023. [2](#), [3](#), [4](#), [7](#)
- [36] Chin-Yew Lin. Rouge: A package for automatic evaluation of summaries. In *Annual Meeting of the Association for Computational Linguistics*, 2004. [13](#)
- [37] Haotian Liu, Chunyuan Li, Yuheng Li, and Yong Jae Lee. Improved baselines with visual instruction tuning. *ArXiv*, abs/2310.03744, 2023. [7](#)
- [38] Haotian Liu, Chunyuan Li, Qingyang Wu, and Yong Jae Lee. Visual instruction tuning. *ArXiv*, abs/2304.08485, 2023. [1](#), [2](#), [4](#)
- [39] Jiawei Liu, Cheng Yang, Zhiyuan Lu, Junze Chen, Yibo Li, Mengmei Zhang, Ting Bai, Yuan Fang, Lichao Sun, Philip S. Yu, and Chuan Shi. Towards graph foundation models: A survey and beyond. *ArXiv*, abs/2310.11829, 2023. [2](#)
- [40] Peng Liu, Yiming Ren, and Zhixiang Ren. Git-mol: A multi-modal large language model for molecular science with graph, image, and text. *ArXiv*, abs/2308.06911, 2023. [2](#), [4](#), [6](#), [7](#)
- [41] Shengchao Liu, Hanchen Wang, Weiyang Liu, Joan Lasenby, Hongyu Guo, and Jian Tang. Pre-training molecular graph representation with 3d geometry. *ArXiv*, abs/2110.07728, 2021. [2](#), [5](#), [6](#), [7](#), [8](#)
- [42] Shengchao Liu, Weili Nie, Chengpeng Wang, Jiarui Lu, Zhuoran Qiao, Ling Liu, Jian Tang, Chaowei Xiao, and Anima Anandkumar. Multi-modal molecule structure-text model for text-based retrieval and editing. *ArXiv*, abs/2212.10789, 2022. [2](#), [4](#), [5](#)
- [43] Zequn Liu, W. Zhang, Yingce Xia, Lijun Wu, Shufang Xie, Tao Qin, Ming Yang Zhang, and Tie-Yan Liu. Molxpt: Wrapping molecules with text for generative pre-training. *ArXiv*, abs/2305.10688, 2023. [6](#), [7](#)
- [44] Jieyu Lu and Yingkai Zhang. Unified deep learning model for multitask reaction predictions with explanation. *Journal of chemical information and modeling*, 2022. [2](#)
- [45] Jieyu Lu and Yingkai Zhang. Unified deep learning model for multitask reaction predictions with explanation. *Journal of chemical information and modeling*, 2022. [4](#), [13](#)
- [46] Jiasen Lu, Dhruv Batra, Devi Parikh, and Stefan Lee. Vilbert: Pretraining task-agnostic visiolinguistic representations for vision-and-language tasks. In *Neural Information Processing Systems*, 2019. [2](#)
- [47] Gen Luo, Yiyi Zhou, Tianhe Ren, Shen Chen, Xiaoshuai Sun, and Rongrong Ji. Cheap and quick: Efficient vision-language instruction tuning for large language models. *ArXiv*, abs/2305.15023, 2023. [2](#)
- [48] Yi Luo, Kai Yang, Massimo Hong, Xingyi Liu, and Zaiqing Nie. Molfm: A multimodal molecular foundation model. *ArXiv*, abs/2307.09484, 2023. [2](#), [4](#), [6](#), [7](#), [13](#)
- [49] Yi Luo, Jiahuan Zhang, Siqi Fan, Kai Yang, Yushuai Wu, Mu Qiao, and Zaiqing Nie. Biomedgpt: Open multimodal generative pre-trained transformer for biomedicine. *ArXiv*, abs/2308.09442, 2023. [2](#), [3](#), [4](#), [6](#), [7](#)
- [50] OpenAI. "chatgpt: A language model for conversational ai. 2023. [1](#), [2](#)
- [51] OpenAI. Gpt-4 technical report. *ArXiv*, abs/2303.08774, 2023. [2](#)
- [52] Long Ouyang, Jeff Wu, Xu Jiang, Diogo Almeida, Carroll L. Wainwright, Pamela Mishkin, Chong Zhang, Sandhini Agarwal, Katarina Slama, Alex Ray, John Schulman, Jacob Hilton, Fraser Kelton, Luke E. Miller, Maddie Simens, Amanda Askell, Peter Welinder, Paul Francis Christiano, Jan Leike, and Ryan J. Lowe. Training language models to follow instructions with human feedback. *ArXiv*, abs/2203.02155, 2022. [2](#)
- [53] Kishore Papineni, Salim Roukos, Todd Ward, and Wei-Jing Zhu. Bleu: a method for automatic evaluation of machine translation. In *Proceedings of the 40th Annual Meeting on Association for Computational Linguistics - ACL '02*, 2001. [13](#)
- [54] Renjie Pi, Jiahui Gao, Shizhe Diao, Rui Pan, Hanze Dong, Jipeng Zhang, Lewei Yao, Jianhua Han, Hang Xu, and Lingpeng Kong Tong Zhang. Detgpt: Detect what you need via reasoning. *ArXiv*, abs/2305.14167, 2023. [2](#)
- [55] Alec Radford, Jong Wook Kim, Chris Hallacy, Aditya Ramesh, Gabriel Goh, Sandhini Agarwal, Girish Sastry, Amanda Askell, Pamela Mishkin, Jack Clark, Gretchen Krueger, and Ilya Sutskever. Learning transferable visual models from natural language supervision. In *International Conference on Machine Learning*, 2021. [2](#), [4](#)

- [56] Colin Raffel, Noam M. Shazeer, Adam Roberts, Katherine Lee, Sharan Narang, Michael Matena, Yanqi Zhou, Wei Li, and Peter J. Liu. Exploring the limits of transfer learning with a unified text-to-text transformer. *J. Mach. Learn. Res.*, 21: 140:1–140:67, 2019. **1**
- [57] Raghunathan Ramakrishnan, Pavlo O. Dral, Pavlo O. Dral, Matthias Rupp, and O. Anatole von Lilienfeld. Quantum chemistry structures and properties of 134 kilo molecules. *Scientific Data*, 1, 2014. **13**
- [58] Raghunathan Ramakrishnan, Pavlo O Dral, Matthias Rupp, and O Anatole Von Lilienfeld. Quantum chemistry structures and properties of 134 kilo molecules. *Scientific data*, 1(1): 1–7, 2014. **5**
- [59] B. Ramsundar, P. Eastman, P. Walters, and V. Pande. *Deep Learning for the Life Sciences: Applying Deep Learning to Genomics, Microscopy, Drug Discovery, and More*. O’Reilly, 2019. **5**
- [60] Ahmet Sureyya Rifaioglu, Heval Atas, Maria Jesus Martin, Rengul Cetin-Atalay, Volkan Atalay, and Tunca Dogan. Recent applications of deep learning and machine intelligence on in silico drug discovery: methods, tools and databases. *Briefings in Bioinformatics*, 20:1878 – 1912, 2018. **1**
- [61] Nadine Schneider, Roger A. Sayle, and Gregory A. Landrum. Get your atoms in order - an open-source implementation of a novel and robust molecular canonicalization algorithm. *Journal of chemical information and modeling*, 55 10:2111–20, 2015. **13**
- [62] Hayal Bulbul Sonmez, Figen Kuloğlu, Koksal Karadag, and Fred Wudl. Terephthalaldehyde- and isophthalaldehyde-based polyspiroacetals. *Polymer Journal*, 44:217–223, 2012. **3**
- [63] Hannes Stärk, D. Beaini, Gabriele Corso, Prudencio Tossou, Christian Dallago, Stephan Gunnemann, and Pietro Lio’. 3d infomax improves gnns for molecular property prediction. In *International Conference on Machine Learning*, 2021. **2**
- [64] Bing Su, Dazhao Du, Zhao-Qing Yang, Yujie Zhou, Jiang-meng Li, Anyi Rao, Haoran Sun, Zhiwu Lu, and Ji rong Wen. A molecular multimodal foundation model associating molecule graphs with natural language. *ArXiv*, abs/2209.05481, 2022. **2, 6, 7, 13**
- [65] Jiabin Tang, Yuhao Yang, Wei Wei, Lei Shi, Lixin Su, Suqi Cheng, Dawei Yin, and Chao Huang. Graphgpt: Graph instruction tuning for large language models. *ArXiv*, abs/2310.13023, 2023. **2**
- [66] Rohan Taori, Ishaan Gulrajani, Tianyi Zhang, Yann Dubois, Xuechen Li, Carlos Guestrin, Percy Liang, and Tatsunori B. Hashimoto. Stanford alpaca: An instruction-following llama model. [https://github.com/tatsu-lab/stanford\\_alpaca](https://github.com/tatsu-lab/stanford_alpaca), 2023. **6, 7**
- [67] Ross Taylor, Marcin Kardas, Guillem Cucurull, Thomas Scialom, Anthony S. Hartshorn, Elvis Saravia, Andrew Poulton, Viktor Kerkez, and Robert Stojnic. Galactica: A large language model for science. *ArXiv*, abs/2211.09085, 2022. **5, 6**
- [68] Hugo Touvron, Thibaut Lavril, Gautier Izacard, Xavier Martinet, Marie-Anne Lachaux, Timothée Lacroix, Baptiste Rozière, Naman Goyal, Eric Hambro, Faisal Azhar, Aurelien Rodriguez, Armand Joulin, Edouard Grave, and Guillaume Lample. Llama: Open and efficient foundation language models. *ArXiv*, abs/2302.13971, 2023. **2, 4, 7, 14**
- [69] Sheng Wang, Yuzhi Guo, Yuhong Wang, Hongmao Sun, and Junzhou Huang. Smiles-bert: Large scale unsupervised pre-training for molecular property prediction. *Proceedings of the 10th ACM International Conference on Bioinformatics, Computational Biology and Health Informatics*, 2019. **2**
- [70] Wen Wang, Zhe Chen, Xiaokang Chen, Jiannan Wu, Xizhou Zhu, Gang Zeng, Ping Luo, Tong Lu, Jie Zhou, Y. Qiao, and Jifeng Dai. Visionllm: Large language model is also an open-ended decoder for vision-centric tasks. *ArXiv*, abs/2305.11175, 2023. **2**
- [71] Weihang Wang, Qingsong Lv, Wenmeng Yu, Wenyi Hong, Ji Qi, Yan Wang, Junhui Ji, Zhuoyi Yang, Lei Zhao, Xixuan Song, Jiazheng Xu, Bin Xu, Juanzi Li, Yuxiao Dong, Ming Ding, and Jie Tang. Cogvlm: Visual expert for pretrained language models. *ArXiv*, abs/2311.03079, 2023. **3**
- [72] Yuyang Wang, Jianren Wang, Zhonglin Cao, and Amir Barati Farimani. Molecular contrastive learning of representations via graph neural networks. *Nature Machine Intelligence*, 4: 279 – 287, 2021. **2**
- [73] Jinmao Wei, Xiao-Jie Yuan, Qinghua Hu, and Shuqin Wang. A novel measure for evaluating classifiers. *Expert Syst. Appl.*, 37:3799–3809, 2010. **4, 13**
- [74] Jason Wei, Maarten Bosma, Vincent Zhao, Kelvin Guu, Adams Wei Yu, Brian Lester, Nan Du, Andrew M. Dai, and Quoc V. Le. Finetuned language models are zero-shot learners. *ArXiv*, abs/2109.01652, 2021. **2**
- [75] David Weininger. Smiles, a chemical language and information system. 1. introduction to methodology and encoding rules. *J. Chem. Inf. Comput. Sci.*, 28:31–36, 1988. **4**
- [76] Chaoyi Wu, Xiaoman Zhang, Ya Zhang, Yanfeng Wang, and Weidi Xie. Pmc-llama: Towards building open-source language models for medicine. 2023. **3**
- [77] Zhenqin Wu, Bharath Ramsundar, Evan N. Feinberg, Joseph Gomes, Caleb Geniesse, Aneesh S. Pappu, Karl Leswing, and Vijay S. Pande. Moleculenet: A benchmark for molecular machine learning. *arXiv: Learning*, 2017. **4, 5, 6, 13**
- [78] Canwen Xu, Daya Guo, Nan Duan, and Julian McAuley. Baize: An open-source chat model with parameter-efficient tuning on self-chat data. *ArXiv*, abs/2304.01196, 2023. **6, 7**
- [79] Keyulu Xu, Weihua Hu, Jure Leskovec, and Stefanie Jegelka. How powerful are graph neural networks? *ArXiv*, abs/1810.00826, 2018. **5**
- [80] Rui Yang, Lin Song, Yanwei Li, Sijie Zhao, Yixiao Ge, Xiu Li, and Ying Shan. Gpt4tools: Teaching large language model to use tools via self-instruction. *ArXiv*, abs/2305.18752, 2023. **2**
- [81] Qinghao Ye, Haiyang Xu, Guohai Xu, Jiabo Ye, Ming Yan, Yi Zhou, Junyan Wang, Anwen Hu, Pengcheng Shi, Yaya Shi, Chenliang Li, Yuanhong Xu, Hehong Chen, Junfeng Tian, Qiang Qi, Ji Zhang, and Feiyan Huang. mplug-owl: Modularization empowers large language models with multimodality. *ArXiv*, abs/2304.14178, 2023. **1, 2, 3, 4**
- [82] Shukang Yin, Chaoyou Fu, Sirui Zhao, Ke Li, Xing Sun, Tong Xu, and Enhong Chen. A survey on multimodal large language models. *ArXiv*, abs/2306.13549, 2023. **2**

- [83] Yuning You, Tianlong Chen, Yongduo Sui, Ting Chen, Zhangyang Wang, and Yang Shen. Graph contrastive learning with augmentations. *ArXiv*, abs/2010.13902, 2020. [2](#), [6](#)
- [84] Zheni Zeng, Yuan Yao, Zhiyuan Liu, and Maosong Sun. A deep-learning system bridging molecule structure and biomedical text with comprehension comparable to human professionals. *Nature Communications*, 13, 2022. [2](#), [6](#)
- [85] Xiaoman Zhang, Chaoyi Wu, Ziheng Zhao, Weixiong Lin, Ya Zhang, Yanfeng Wang, and Weidi Xie. Pmc-vqa: Visual instruction tuning for medical visual question answering. *ArXiv*, abs/2305.10415, 2023. [2](#)
- [86] Gengmo Zhou, Zhifeng Gao, Qiankun Ding, Hang Zheng, Hongteng Xu, Zhewei Wei, Linfeng Zhang, and Guolin Ke. Uni-mol: A universal 3d molecular representation learning framework. In *International Conference on Learning Representations*, 2023. [5](#), [6](#)
- [87] Deyao Zhu, Jun Chen, Xiaoqian Shen, Xiang Li, and Mohamed Elhoseiny. Minigt-4: Enhancing vision-language understanding with advanced large language models. *ArXiv*, abs/2304.10592, 2023. [1](#), [2](#), [3](#)

This supplementary material includes additional details and results not included in the main paper due to page limitations. The items included are as follows:

- Elaboration on task definitions and datasets in Sec A.
- Further details regarding evaluation metrics in Sec B.
- Illustrative samples of instructions for each task (refer to Tab 7) and examples of the process for constructing prompts in the context of few-shot in-context learning (refer to Fig 8).
- Additional results for each task and several challenging cases in Sect. C.

## A. Tasks Definition and Dataset Details

**Property Prediction.** Molecular Property Prediction involves the forecasting or estimation of the biophysical and chemical properties of a molecule. In this work, our emphasis lies on three binary classification tasks sourced from the MoleculeNet benchmark (BBBP, BACE, and HIV) [77], and three regression tasks concentrating on the quantum properties of molecules from the QM9 [57] dataset.

**Molecule Description Generation.** Generating molecular descriptions involves compiling a detailed overview of a molecule’s structure, properties, activities, and functions. This process aids chemists and biologists by swiftly providing crucial molecular insights for their research. Our data collection involves the extraction of molecular text annotations from PubChem [29]. Leveraging PubChem’s **Power User Gateway** [28], we retrieve abstracts of compound records in XML format. Subsequently, we extracted valid molecular description texts identified by unique PubChem Chemical Identifiers (CIDs), filtering out SMILES strings with syntactic errors or deviations from established chemical principles. Furthermore, we utilize the ChEBI-20 dataset [17] for downstream tasks in molecule description generation, comprising 33,010 molecule description pairs divided into 80% for training, 10% for validation and 10% for testing. To prevent data leakage, compounds in the PubChem text annotations that coincide with the ChEBI-20 test split are excluded.

**Forward Reaction Prediction.** Predicting the forward reaction involves anticipating the probable product(s) of a chemical reaction based on given reactants and reagents. For this task, we utilize the forward-reaction-prediction dataset from [22], comprising 138,768 samples sourced from the USPTO dataset [73]. Each entry includes reactants and reagents separated by ‘.’ within the instruction and with the output product.

**Reagent Prediction.** Reagent prediction identifies the substances necessary for a chemical reaction, helping to discover new types of reactions and optimal conditions. We

use the reagent Prediction data from [22], sourced from the USPTO\_500MT dataset [45]. Each entry features a chemical reaction indicated as “reactants >> product”, with the output indicating the reagents involved in the reaction.

**Retrosynthesis Prediction.** Retrosynthetic analysis in organic chemistry reverses engineering by tracing potential synthesis routes from the target compound backward. This strategy is vital for efficient synthesis of complex molecules and for fostering innovation in pharmaceuticals and materials. For this task, we also used the dataset from [22], which is sourced from USPTO\_500MT. The data organize inputs as products and outputs as reactants separated by ‘.’ for each compound.

## B. Evaluate Metrics

**Molecule Description Generation Metric.** Following [18], NLP metrics such as BLEU [53], ROUGE [36] and METEOR [5] are used to assess the proximity of generated descriptions to the truth of the ground. Specifically, these metrics are tested on the ChEBI-20 test dataset. In our experiments, we observed that after 50 epochs of finetuning on the training split, the metrics tend to converge, differing from previous approaches that often involved fine-tuning for over 100 epochs [18, 48, 64].

**Molecule Generation Metric.** In chemical reaction tasks, we view it as akin to a text-based molecule generation task. Initially, we employ RDKit to validate the chemical validity of the generated results, ensuring their “validity”. Subsequently, we gauge the sequential proximity between the generated sequence and the ground truth using NLP metrics such as BLEU, Exact Match scores, and Levenshtein distance. Additionally, we present performance based on molecule-specific metrics that assess molecular similarity, encompassing RDKit, MACCS [16], and Morgan [61] fingerprints similarity.

TASK	INSTRUCTION
Alignment Pretrain	Instruction: <i>Provide a brief overview of this molecule.</i>    [Optional: The compound SELFIES sequence is: SELFIES] Output: <i>The molecule is a non-proteinogenic alpha-amino acid that is ...</i>
Property Prediction (Regression)	Instruction: <i>Could you give me the LUMO energy value of this molecule?</i>    [Optional: The compound SELFIES sequence is: SELFIES] Output: <i>0.0576</i>
Property Prediction (Classification)	Instruction: <i>Evaluate whether the given molecule is able to enter the blood-brain barrier.</i>    [Optional: The compound SELFIES sequence is: SELFIES] Output: <i>Yes</i>
Molecule Description Generation	Instruction: <i>Could you give me a brief overview of this molecule?</i>    [Optional: The compound SELFIES sequence is: SELFIES] Output: <i>The molecule is a fatty acid ester obtained by ...</i>
Forward Prediction	Instruction: <i>Based on the given reactants and reagents, suggest a possible product.</i>    <REACTANT A>.<REACTANT B>...<REAGENT A>.<REAGENT B>... Output: SELFIES of product
Retrosynthesis	Instruction: <i>Please suggest potential reactants used in the synthesis of the provided product.</i>    SELFIES of product Output: <REACTANT A>.<REACTANT B>...<REAGENT A>.<REAGENT B>...
Reagent Prediction	Instruction: <i>Can you provide potential reagents for the following chemical reaction?</i>    <REACTANT A>.<REACTANT B>...<REAGENT A>.<REAGENT B>... >> <PRODUCTs> Output: SELFIES of reagent

Table 7. Examples of instruction samples for each task. || means concatenate along the token dimension.

```
messages = [ {"role": "system", "content": f"" "You're acting as a molecule property prediction assistant. You'll be given SMILES of molecules and you need to make binary classification with a return result only in "True" or "False".
```

**The background of the dataset and task is shown below:**

The Blood-brain barrier penetration (BBBP) dataset comes from a recent study on the modeling and prediction of barrier permeability. As a membrane separating circulating blood and brain extracellular fluid, the blood-brain barrier blocks most drugs, hormones, and neurotransmitters. Thus penetration of the barrier forms a long-standing issue in the development of drugs targeting the central nervous system.

We provide several examples for this binary classification task:

###

Instruction: Predict whether the given compound has barrier permeability. Return True or False.

SMILES: CCC(=O)C(CC(C)N(C)C)(c1cccc1)c2cccc2

Output: True

###

###

Instruction: Predict whether the provided compound exhibits barrier permeability. Return True or False.

SMILES: c1cc2c(cc(CC3=CNC(=NC3=O)NCCSCc3oc(cc3)CN(C)C)cc2)cc1

Output: False

###

...

Given the following instructions and SMILES, return your prediction result:

Instruction: Predict whether the provided compound exhibits barrier permeability. Return True or False.

SMILES: TARGET SMILES

```
"" "}
```

```
]
```

Table 8. An illustration of the few-shot in-context-learning prompt construction process for Llama [20, 68] / Vicuna [9] models in property prediction tasks.

## C. More Examples

### C.1. More Results of Molecule Description Generation

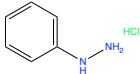
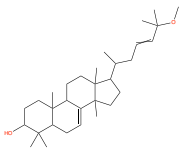
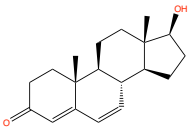
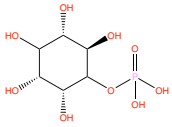
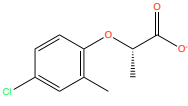
	Mol-Instruction	InstructMol	Ground Truth
	The molecule is the potassium salt of acetic acid. It has a role as a buffer. It is a potassium salt and an acetate salt. It contains an acetate.	The molecule is a potassium salt that is the monokis salt of carbonic acid. It has a role as a buffer. It is a carbonate salt and a potassium salt. It contains a carbonate.	The molecule is the potassium salt of formic acid. It has a role as a buffer. It is a potassium salt and a one-carbon compound. It derives from a formic acid.
CID: 2735122			
	The molecule is an organic molecular entity.	The molecule is a hydrochloride salt resulting from the reaction of equimolar amounts of 1-nitrobenzene and hydrogen chloride. It has a role as a mutagen. It contains a 1-nitrobenzene(2+).	The molecule is a hydrochloride resulting from the reaction of equimolar amounts of phenylhydrazine and hydrogen chloride. It contains a phenylhydrazine.
CID: 60962			
	The molecule is a triterpenoid.	The molecule is a tirucallane triterpenoid that is (13alpha,14beta,17alpha,20S,23E)-lanosta-7,23-diene substituted by an oxo group at position 3 and a methoxy group at position 25. It has been isolated from the stem and stem barks of Cornus walteri. It has a role as a plant metabolite. It is an ether, a tirucallane triterpenoid and a secondary alcohol.	The molecule is a tirucallane triterpenoid that is (13alpha,14beta,17alpha,20S,23E)-lanosta-7,23-diene substituted by a beta-hydroxy group at position 3 and a methoxy group at position 25. It has been isolated from the stem and stem barks of Cornus walteri. It has a role as a plant metabolite. It is a tirucallane triterpenoid, an ether and a secondary alcohol.
CID: 50994221			
	The molecule is an organic thiophosphate.	The molecule is an organic thiophosphate that is O,O-dimethyl hydrogen phosphorothioate in which the hydrogen of the hydroxy group has been replaced by a 3,5,6-trichloropyridin-2-yl group. It has a role as an agrochemical, an EC 3.1.1.7 (acetylcholinesterase) inhibitor and an environmental contaminant. It is an organic thiophosphate, a chloropyridine and an organochlorine pesticide.	The molecule is an organic thiophosphate that is O,O-diethyl hydrogen phosphorothioate in which the hydrogen of the hydroxy group has been replaced by a 3,5,6-trichloropyridin-2-yl group. It has a role as an EC 3.1.1.7 (acetylcholinesterase) inhibitor, an agrochemical, an EC 3.1.1.8 (cholinesterase) inhibitor, an environmental contaminant, a xenobiotic, an acaricide and an insecticide. It is an organic thiophosphate and a chloropyridine.
CID: 2730			
	The molecule is a natural product found in Homo sapiens with data available.	The molecule is a 17beta-hydroxy steroid that is testosterone in which the 17beta hydrogen is replaced by a methyl group. It has a role as an androgen. It is a 3-oxo-Delta(4) steroid and a 17beta-hydroxy steroid. It derives from a testosterone.	The molecule is a 17beta-hydroxy steroid that is testosterone that contains an additional double bond between positions 6 and 7. It is a 3-oxo-Delta(4) steroid, a 17beta-hydroxy steroid and an enone. It derives from a testosterone.
CID: 17209			
	The molecule is a metabolite found in or produced by Escherichia coli (strain K12, MG1655).	The molecule is a myo-inositol monophosphate. It has a role as an algal metabolite and a mouse metabolite. It derives from a myo-inositol. It is a conjugate acid of a 1D-myo-inositol 4-phosphate(2-).	The molecule is an inositol having myo-configuration substituted at position 1 by a phosphate group. It has a role as a human metabolite, an Escherichia coli metabolite and a mouse metabolite. It derives from a myo-inositol. It is a conjugate acid of a 1D-myo-inositol 1-phosphate(2-).
CID: 107737			
	The molecule is a monocarboxylic acid anion resulting from the removal of a proton from the carboxy group of (R)-imazamox. It is a conjugate base of a (R)-imazamox. It is an enantiomer of a (S)-imazamox(1-)	The molecule is a monocarboxylic acid anion resulting from the removal of a proton from the carboxy group of (S)-methyl 2-(4-chloro-2-methylphenoxy)acetate. It is a conjugate base of a (S)-methyl 2-(4-chloro-2-methylphenoxy)acetate. It is an enantiomer of a (R)-methyl 2-(4-chloro-2-methylphenoxy)acetate(1-).	The molecule is a monocarboxylic acid anion that is the conjugate base of (S)-2-(4-chloro-2-methylphenoxy)propanoic acid, obtained by deprotonation of the carboxy group. It is a conjugate base of a (S)-mecoprop. It is an enantiomer of a (R)-2-(4-chloro-2-methylphenoxy)propanoate.
CID: 107737			

Figure 5. More examples of molecule description generation task on ChEBI-20 [17] test set. We include Mol-Instruction [22] as the baseline. CID [1]: PubChem Compound Identification, a non-zero integer PubChem accession identifier for a unique chemical structure.

## C.2. More Results of Forward Reaction Prediction

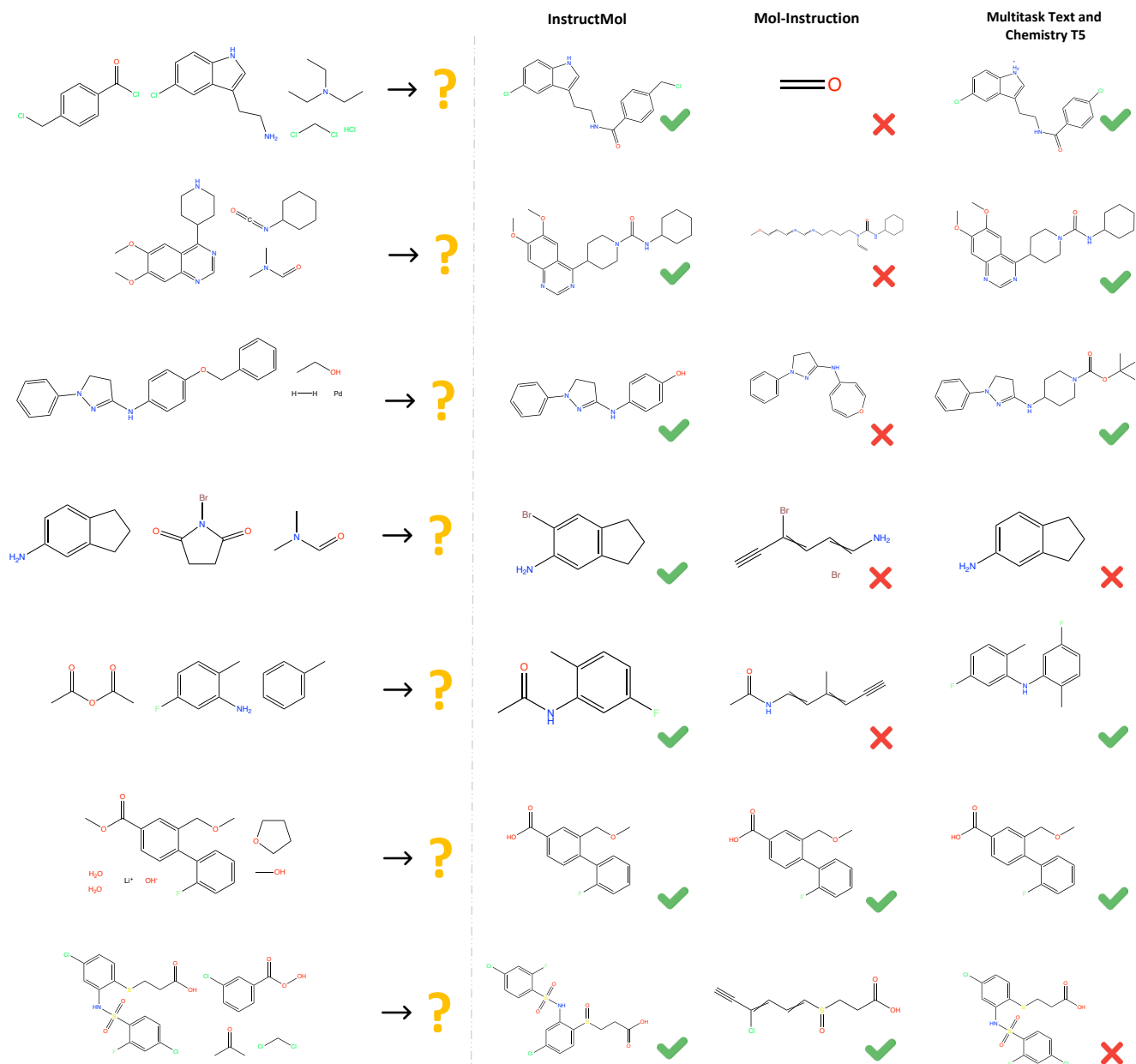


Figure 6. More examples of forward reaction prediction task. We include Mol-Instruction [22] and Multitask-Text-and-Chemistry-T5 [11] as baselines.

### C.3. More Results of Reagent Prediction

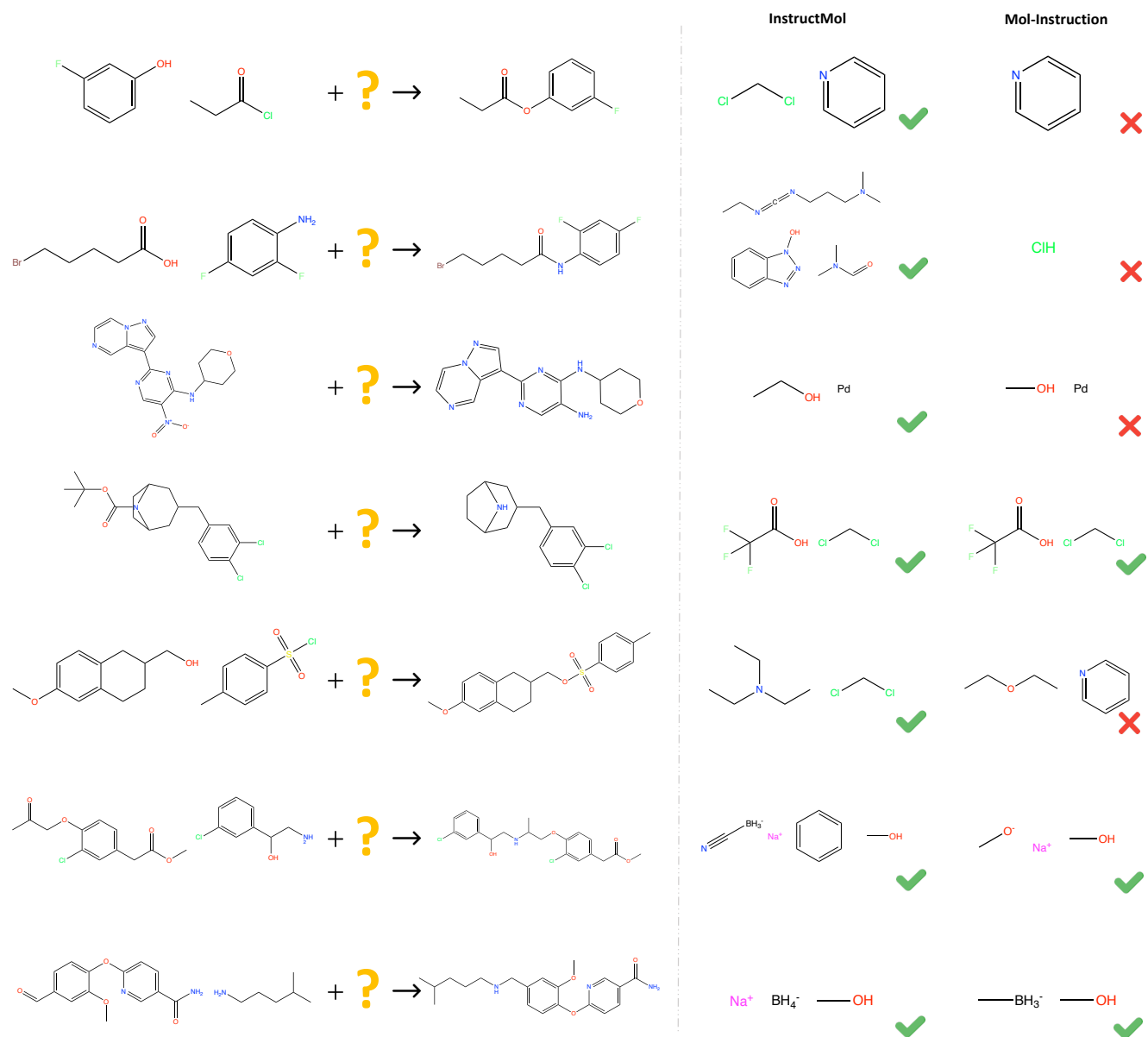


Figure 7. More examples of the reagent prediction task. We include Mol-Instruction [22] as the baseline.

## C.4. More Results of Retrosynthesis Prediction

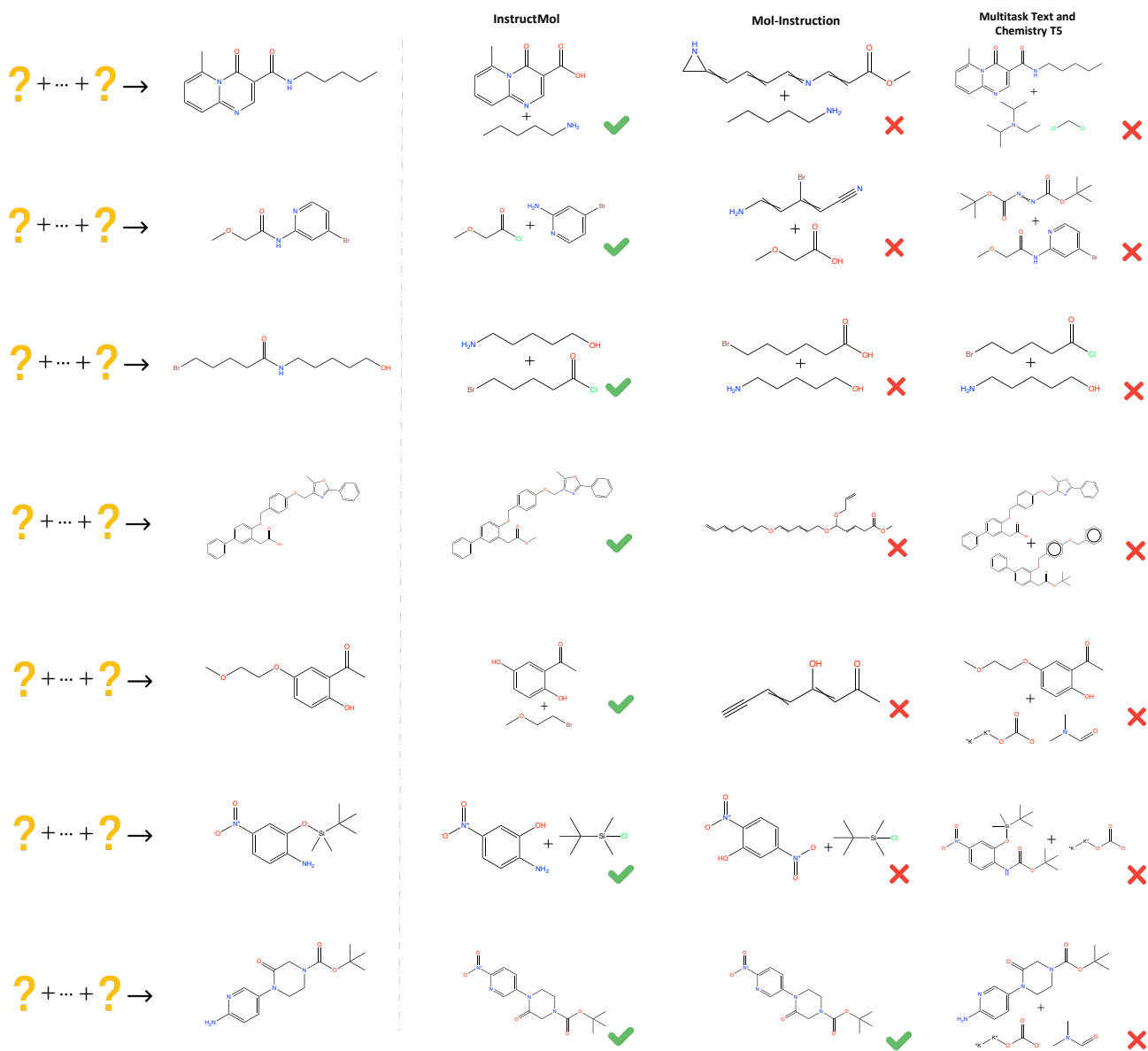


Figure 8. More examples of the retrosynthesis prediction task. We include Mol-Instruction [22] and Multitask-Text-and-Chemistry-T5 [11] as baselines.

## C.5. Difficult Cases

We showcase cases with misalignment to the ground truth, along with RDKit fingerprint similarity results in Fig. 9. The complexity of chemical reaction compounds makes the task more challenging. In addressing this limitation, our future approach involves concatenating graph tokens from multiple molecules involved in the same reaction with text tokens to simplify the complexity of the input sequence. Moreover, we are considering employing separate tokenization and embedding for distinct modalities to ensure the semantic accuracy of the tokenized results.

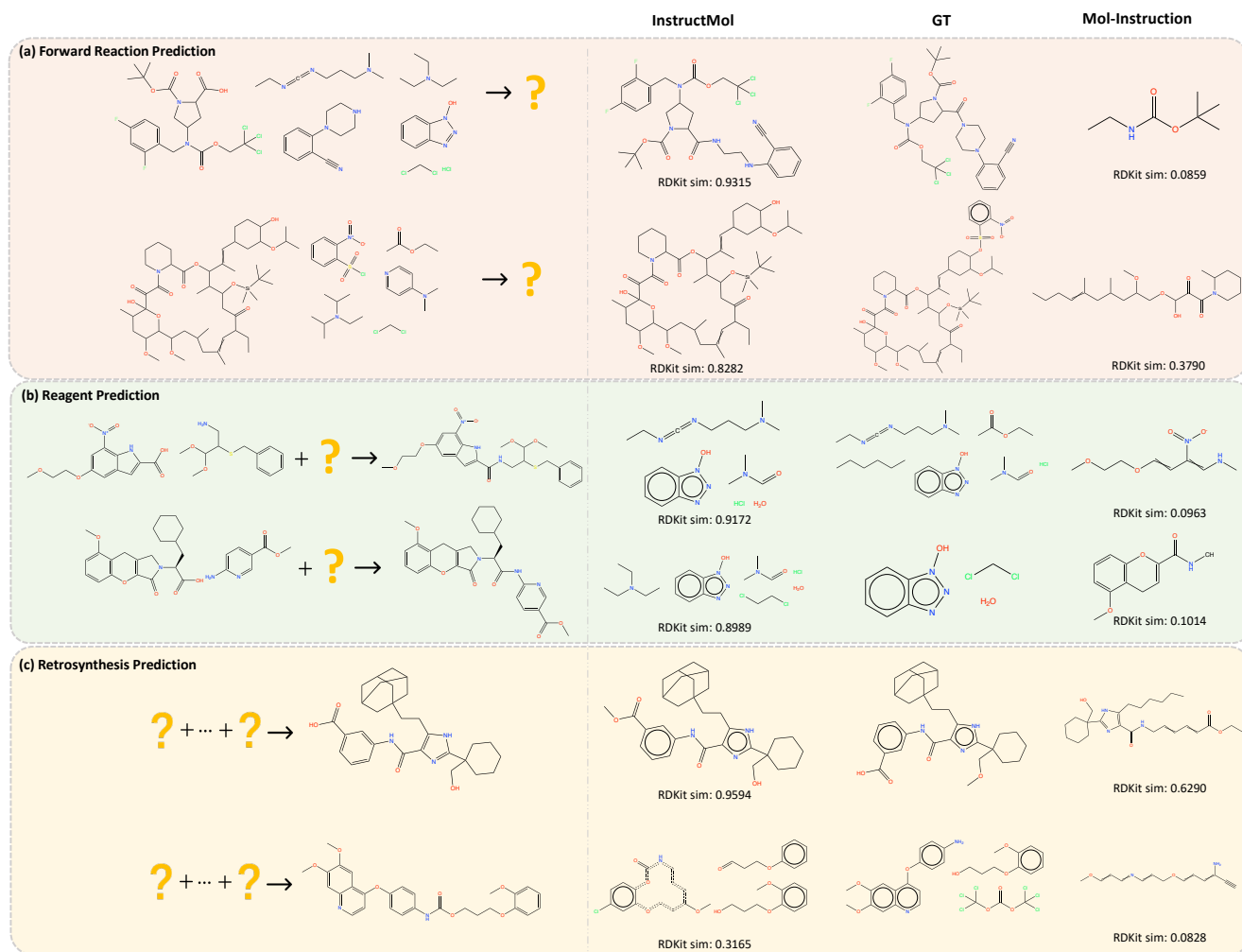


Figure 9. We present several cases with a certain degree of misalignment compared to the ground truth, accompanied by RDKit fingerprint similarity results relative to the ground truth. Due to the heightened complexity of compounds involved in chemical reactions, the difficulty of the task increases, leading to the poor performance of Mol-Instructions [22].